Soil & Tillage Research 205 (2021) 104748

Contents lists available at ScienceDirect

Soil & Tillage Research

journal homepage: www.elsevier.com/locate/still

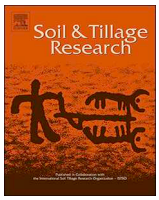

The impact of various mulch types on soil properties controlling water regime of the Haplic Fluvisol

Lenka Pavlů[a,*], Radka Kodešová[a], Miroslav Fér[a], Antonín Nikodem[a], František Němec[b], Radek Prokeš[c]

[a] Czech University of Life Sciences Prague, Department of Soil Science and Soil Protection, Kamýcká 129, CZ-16500, Prague Suchdol, Czech Republic
[b] Charles University, Department of Surface and Plasma Science, Ovocný trh 5, CZ-11636, Prague 1, Czech Republic
[c] Czech University of Life Sciences Prague, Department of Landscape Architecture, Kamýcká 129, CZ-16500, Prague Suchdol, Czech Republic

ARTICLE INFO

Keywords:
Mulches
Soil water and thermal regimes
Aggregate stability
Soil chemical properties
Soil hydraulic properties

ABSTRACT

A long-term application of various mulch materials may lead to changes in certain soil properties, which mostly remain unreviewed. Therefore, our study focused on the mulch effect on a larger group of Haplic Fluvisol properties. The experiment was performed on 27 perennial patches covered by eight different mulch materials (bark chips, wood chips, wheat straw, cardboard, paper foil, decomposable matting, nonwoven fabric covered by bark chips, and crushed basalt) and control patches without any mulch during the 4 year period.

The highest daily ranges of soil temperature were found in control patches without mulch, lower temperature ranges below foils mulches, and the lowest below organic mulches. Mulches preserved water storage in soil mainly during spring before vegetation integration and after perennials' cutting. Organic carbon content (C_{ox}), aggregate stability, and pH mostly did not show any trends over time, except for C_{ox} and aggregate stability from patches with bark or wood chips and wheat straw. In these cases, decomposed organic matter significantly increased both properties. On the other hand, the soil hydraulic properties (mostly due to no-till practice) considerably changed in all patches. The saturated and residual water contents, saturated hydraulic conductivity, and reciprocal of the air-entry pressure head increased. Correspondingly, the bulk density decreased. Soil water retention curves from the patches with bark or wood chips were more gradual than those from other patches, which indicates higher water retention capacity for lower pressure heads. However, the physical quality of soils under organic mulches expressed by the slope at the retention curve inflection point was lower than that for other scenarios. Readily available water under organic mulches was also lower than that for other setups. This suggests that organic mulches have largest impacts on soil conditions, which can be either favourable or adverse.

1. Introduction

Mulching is a known technology used in agriculture and garden systems for centuries. The reasons for mulch application are mostly weed reduction and improving the water or thermic soil regime. Additionally, mulches are used in anti-erosion soil protection (Nzeyimana et al., 2017; Rees et al., 2002). At present, a wide variety of mulch materials exist, including polyethylene foils, polypropylen nonwoven fabrics, biodegradable plastic foils, paper films, organic mulches, such as straw or wood chips, and also gravels (e.g., Al-Shammary et al., 2020; Kasirajan and Ngouajio, 2012; Yang et al., 2020). Some mulch types are used in open or greenhouse agriculture systems. Wood chips or gravels are preferred in gardening. Each of these materials has a specific effect on soil.

Detailed discussions of polyethylene foil's effect on yield quality, pest management, soil porosity, water transport, and soil organic matter composition and stability were presented by Steinmetz et al. (2016), who identified certain reasons for farmers to apply plastic foils in agriculture, i.e., soil water saving and pest control, but also identified a number of risks and the less beneficial effects of plastic mulching. These include the persistence of unrecovered plastic foil in soil, the shift of the edaphic biocoenosis, and an increased risk of mycotoxin formation in soil. A significant negative effect of plastic foils on soil bacterial richness was documented by Li et al. (2019). When plastic mulch is

* Corresponding author.
E-mail addresses: pavlu@af.czu.cz (L. Pavlů), kodesova@af.czu.cz (R. Kodešová), mfer@af.czu.cz (M. Fér), nikodem@af.czu.cz (A. Nikodem), frantisek.nemec@mff.cuni.cz (F. Němec), radek.proky@seznam.cz (R. Prokeš).

https://doi.org/10.1016/j.still.2020.104748
Received 2 January 2020; Received in revised form 2 July 2020; Accepted 14 July 2020

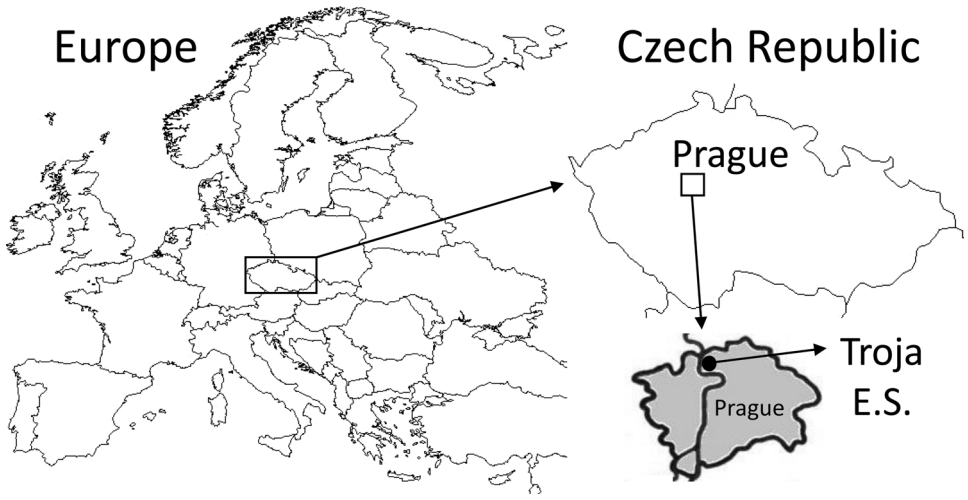

Fig. 1. Experiment localization (experiment station–E.S.).

embedded in soil, it undergoes numerous processes, and is converted into microplasts (Blasing and Amelung, 2018). Together with the microplastics themselves, organic and inorganic pollutants absorbed during their travel are also accumulated in soils (Wang et al., 2019). Subsequently, microplastics and related pollutants can have adverse effects on flora and fauna.

An alternative solution for reducing waste from plastic mulches is to develop degradable mulches. Kasirajan and Ngouajio (2012), in their review, compared polyethylene foils with biodegradable and photodegradable plastic mulches. Biodegradable polymers (especially those derived from plant sources) begin their lifecycle as renewable resources, usually in the form of starch or cellulose. Environmental degradability is a process that is strongly affected by the biotic and abiotic conditions to which they are exposed. The breakdown of degradable plastics has been categorized into disintegration and mineralization. Biodegradable plastics are broken down by naturally occurring microorganisms and ultimately converted to carbon dioxide and water under aerobic conditions. Various biodegradable mulches have also been listed and compared by Yang et al. (2020). A biopolymer combines characteristics of the plastic materials with a biodegradation rate analogous to paper, which is also often used as degradable mulch. Saglam et al. (2017) showed that both biodegradable paper and biodegradable plastic mulches reduced evaporation by restricting water and vapour flow across the soil–atmosphere interface, and thereby conserved water in the root zone. However, the water conservation effect of biodegradable paper and biodegradable plastic mulch depends on their disintegration rates during the growing season (Moreno et al., 2017).

Natural mulches help in maintaining soil organic matter and provide a food source and living space for soil biota (Doran, 1980; Kader et al., 2017a). Cereal straw is the most common organic mulching material (Kasirajan and Ngouajio, 2012). Natural mulches do not always provide adequate weed control. They may carry weed seeds and often retard soil warming in spring. Straw mulches often contaminate the soil with weed seeds and deplete the seedbed nitrogen due to their high carbon-to-nitrogen (C/N) ratio (Kasirajan and Ngouajio, 2012). Organic materials that have a high C/N ratio, such as grain straw, may temporarily immobilize soil nitrogen as they decompose. Natural mulches are reported to reduce soil temperature and evaporation (Kader et al., 2017b; Subrahmaniyan and Zhou, 2008). Natural mulch cover is effective in reducing soil erosion by water. Furthermore, the effectiveness of mulch cover is also controlled by slope, soil texture, and mulch type (Smets et al., 2008).

Crushed stone, gravel, and sand application is also a traditional mulching technique (Gale et al., 1993) in specific agriculture systems, such as vineyards. In arid and semi-arid regions, gravel mulch is a common and effective substance used to decrease soil surface evaporation and has a long history (Lemon, 1956). Crush stones or gravel with different textures and colours are widely used in garden architecture for their esthetic benefits. The original use of a gravel mulch was to conserve sporadic and limited rainfall and protect soils from erosion. Nachtergaele et al. (1998) and Kodešová et al. (2014) showed the effects of a gravel mulch on soil temperature and on evaporation. Plant roots are protected from low temperatures (even frost) at night or during the spring. The gravel mulch stratum on the soil surface reduced the amount of water loss through evaporation (Qiu et al., 2014), and the soil surface evaporation reduction abilities of gravel mulches were negatively correlated with gravel sizes (Yuan et al., 2009). Xie et al. (2010) compared gravel and sand mulches. They concluded that the small-size particles were better for preserving heat in soil than larger ones with bigger porosity in the mulching layer. Further, the mixed pebble and sand mulch were more effective to conserve soil water than the sole pebble or sand mulch (Ma and Li, 2011).

As we show, many previous studies focused on the mulch effect's yield quality or the water and temperature distribution in soil below a few types of mulch materials. The main novelty of our work is in comparing eight types of mulches, including plastic foils, degradable foils, organic materials, and gravel in one place and evaluating of changes in wide range of soil properties (soil chemical properties, aggregate stability, soil water retention curves, and hydraulic properties) during the 4-year-period. Interrelationships among these properties were also looked for. Our main questions were: (1) Is there any general trend in temporal changes of evaluated soil properties (i.e., similarity in rates of responses to founding different mulch covers in time), or are these trends dependent on mulch type and/or soil property. (2) Is the mulch effect to soil chemical parameters connected directly with parameters characterizing soil structure and hydraulic properties? Are these parameters correlated during the entire period or only for a particular phase? (3) How do the effects of organic or degradable mulch materials differ from undegradable foil and crushed stones?

2. Materials and methods

2.1. Field setup and soil sampling

Our experiment began on the field of the university experimental station in Troja (Prague) (Fig. 1) in 2015 as a multidisciplinary study combining soil science and gardening (perennials surviving studied by other research group) points of view on mulch application. The soil was

Table 1
Mulch types used in the experiment (application time is accented if it varies from spring 2015).

Abbreviation	Description
NMU	Not mulched control patch
CBD	Cardboard (200 g m^2) in three layers
EKC	EkoCover RF; decomposable rain forced paper mulch foil (900 g m^2)
ATE	Agrotex EKO +; biopolymer PLA[a] decomposable matting (150 g m^2)
NFB	Polypropylene nonwoven fabric (50 g m^2) covered by 3 cm bark chips layer
BRK	Bark chips in 10 cm high layer (spring 2015 and 2017)
WCH	Wood chips in 10 cm high layer (spring 2015 and 2017)
STR	Wheat straw in 10 cm high layer (spring 2015 and 2017)
CRS	Crushed stone (basalt 1.5 cm) in the 10 cm high layer

[a] PLA polylactic acid—thermoplastic aliphatic polyester derived from renewable biomass.

described as Haplic Fluvisol (IUSS, 2014) developed on fluvial sediments of the Vltava river. Formerly, the field was commonly cultivated and used for crop production. Before outplanting the perennials (April 2015), five grab and five undisturbed (using 100 cm^3 columns) soil samples were collected from 2 soil layers (0–10 cm and 20–40 cm). An experimental plot was then divided into 27 patches (3 × 1.5 m). Twenty-four patches were covered by eight types of mulch (Tables 1 and 3 replicates for each), and 3 control patches remained uncovered. Perennials (*Geranium sanguineum* 'Ankum´s Pride', *Hemerocallis* 'Stella D´Oro', *Salvia nemorosa* 'Caradonna', *Echinacea purpurea* 'Primadonna Deep Rose', *Coreopsis verticilata* 'Grandiflora', and *Heuchera sanguinea* 'Leuchtkäfer') were outplanted, following the same scheme at each patch. The experimental design (i.e., the patches' situations and the scheme of plant distribution within each patch) is shown in the Appendix A (Fig. A1). The layers of straw, bark, and wood chips were renewed for experimental purposes after two seasons because these materials were largely decomposed. The Cardboard and EkoCover RF foil were also almost completely decomposed after 2 years. In these cases, it was impossible to fill these materials in perennial patches These materials are used in practice when establishing perennial patches. Their anti-weed function is later taken over by the vegetation development. It should be mentioned that various degradable foils and other decomposable materials are also used in fields where agricultural management allows its repositioning (e.g., Al-Shammary et al., 2020; Kasirajan and Ngouajio, 2012; Yang et al., 2020).

The next soil samplings were always carried out after perennials cutting in October 2015, 2016, 2017, and 2018. Disturbed mixed samples from 4 punctures per each patch were collected from the surface layer (0–10 cm) using a gouge auger. Samples for aggregate stability measurements (i.e., undisturbed soil aggregates) were carefully collected separately using a plastic shovel. Undisturbed 100-cm^3 soil samples (2 per patch thus 6 per mulch variant) were taken from the surface layer (0–10 cm) in October 2015 and 2018.

In addition, to gain information about differences in soil water and thermal regimes below different covers (which can affect processes taking place in soils and consequently soil properties), a microclimate data logger called the Temperature-Moisture-Sensor (TMS3) was installed in each patch in October 2015. TMS3 integrates sensors for measuring air, surface and soil (depth of 8 cm) temperature assigned T_3, T_2, and T_1 respectively, as well as soil water content (depth of 1–14 cm). Detail data logger description is presented in Wild et al. (2019). TMS3 sensors for measuring soil water contents (time-domain transmission method, which linearly relates the counts of pulses to volumetric water contents) were calibrated for this soil under laboratory conditions following a procedure similar to the one described by Kodešová et al. (2011b).

2.2. Basic chemicals and physical properties

The soil samples for chemical analyses were dried (in an oven at 40 °C), crushed, and sieved through a 2 mm mesh. The selected soil characteristics were assessed by commonly used methods. Active and exchangeable pH values (pH_{H2O} and pH_{CaCl2}, respectively) were measured potentiometrically by an ion selective electrode (ISO, 10390: 2005). Organic carbon content (Cox) was measured using the rapid dichromate oxidation technique (Sparks, 1996). For soil samples taken before the application of mulches, their particle size distribution was also assessed using the areometric method (CASAGRANDE, 1934). Based on the preliminary analyses of these soil samples (Table 2), soil appertains to a group of sandy loam soils. It is weakly acidic with a relatively low humus content.

2.3. Soil aggregate stability

The air-dried aggregate samples were sieved to extract aggregates with diameters of 2–5 mm that were next used to analyse their stability applying the index of water stable aggregates (WSA) proposed by Nimmo and Perkins (2002). Four grams of air-dried soil aggregates were sieved for 3 min in distilled water (sieve 0.25 mm; 3 replicates). Aggregates remaining on the sieve were then sieved in a $(NaPO_3)_6$ solution (2 g l^{-1}) until only sand particles remained on the sieve. The WSA index was then calculated as

$$WSA = \frac{WDS}{(WDS + WDW)} \quad (1)$$

where WDS is the weight of aggregates dispersed in the $(NaPO_3)_6$ solution, and WDW is the weight of aggregates dispersed in distilled water. Increasing the WSA values indicates an increase in soil aggregate stability.

2.4. Soil hydraulic properties

The undisturbed 100 cm^3 samples were partly immediately analysed or partly stored at 4 °C until their analyses. First, soil hydraulic properties (water retention curve, θ(h), and the hydraulic conductivity function, K(θ)) were measured on these samples using the multistep outflow method (van Dam et al., 1994). Samples were placed into Tempe cells, water saturated, and slowly drained using nine pressure head steps (−10, −30, −50, −100, −170, −250, −350, −500, and −1000 cm) during a 4 week period, and the cumulative outflow in time was measured. The final soil water content (i.e., at a minimum pressure head of −1000 cm) and water balance within the soil sample were used to calculate the points of the soil water retention curve. The observed

Table 2
Average values of soil properties before mulching and planting perennials with standard deviation (5 samples from each layer) (pH in H_2O or $CaCl_2$ soil extract, organic carbon content (C_{ox}) and particle size distribution).

	pH_{H2O} –	pH_{CaCl2} –	C_{ox} %	clay %	silt %	sand %
0–15 cm	6.70 ± 0.10	5.93 ± 0.09	1.68 ± 0.15	13.8 ± 2.6	23.2 ± 0.9	63.0 ± 2.9
20–40 cm	6.83 ± 0.18	5.99 ± 0.18	1.56 ± 0.10	14.1 ± 1.3	26.2 ± 2.5	59.7 ± 2.4

Table 3
The time and the mulch effect on soil properties in whole dataset; results of the main effects analysis of variance: *p*-values of the significance; 95 % LSD, letters a, b, c in the columns represent homogenous groups. (pH in H_2O or $CaCl_2$ soil extract, organic carbon content (C_{ox}), water stable aggregate index (WSA), saturated soil water contents (θ_s), residual soil water contents (θ_r), parameters α and n, saturated hydraulic conductivity (K_s), absolute value of the negative pressure head at the inflection point (h_{inf}), soil water content at inflection point (θ_{inf}), retention curve slope at the inflection point (S_{inf}), bulk density (ρ_d), gravitational water (GW), and readily available water (RAW); NMU–Not mulched control patch; CBD–Cardboard; EKC–EkoCover RF– decomposable foil; ATE–Agrotex; EKO + decomposable matting; NFB–Polypropylene nonwoven fabric covered bark chips layer; BRK–Bark chips; WCH–Wood chips; STR–Wheat straw; CRS–Crushed stone.

	pH_{H2O}	pH_{CaCl2}	C_{ox}	WSA	θ_s	θ_r	α	n	K_s	h_{inf}	θ_{inf}	S_{inf}	ρ_d	GV	RAW
	p-values														
year	< **0.001**	0.007	< **0.001**	0.242	0.113	0.002	0.004	0.763	0.690	0.018	0.026	0.216	0.030	< **0.001**	0.116
mulch	0.014	0.192	< **0.001**	< **0.001**	< **0.001**	0.002	< **0.001**	0.290	< **0.001**	< **0.001**	< **0.001**	0.272	< **0.001**	0.263	0.007
	Homogenous groups														
2015	a	b	a	a	b	b	b	a	b	a	b	a	a	a	a
2016	c	a	a	a											
2017	b	a	b	a											
2018	a	a	a	a	a	a	a	a	a	b	a	a	b	b	a
NMU	ab	ab	b	d	a	cd	c	a	ab	ab	ab	a	bcd	ab	a
CBD	c	ab	b	cd	a	bcd	bc	a	ab	ab	ab	a	bcd	ab	ab
EKC	ab	ab	b	cd	b	cd	c	a	ab	a	c	ab	a	b	ab
ATE	bc	b	b	cd	ab	d	bc	a	ab	ab	bc	ab	bcd	a	ab
NFB	bc	ab	b	b	a	bc	bc	a	b	bc	ab	a	cd	a	bc
BRK	bc	b	a	a	a	a	b	a	ab	abc	a	ab	abc	ab	bc
WCH	a	a	a	a	ab	bc	ab	a	a	c	bc	b	d	ab	c
STR	ab	ab	b	a	ab	cd	bc	a	ab	abc	abc	ab	abcd	ab	ab
CRS	ab	ab	b	bc	ab	ab	bc	a	ab	abc	bc	ab	ab	ab	c

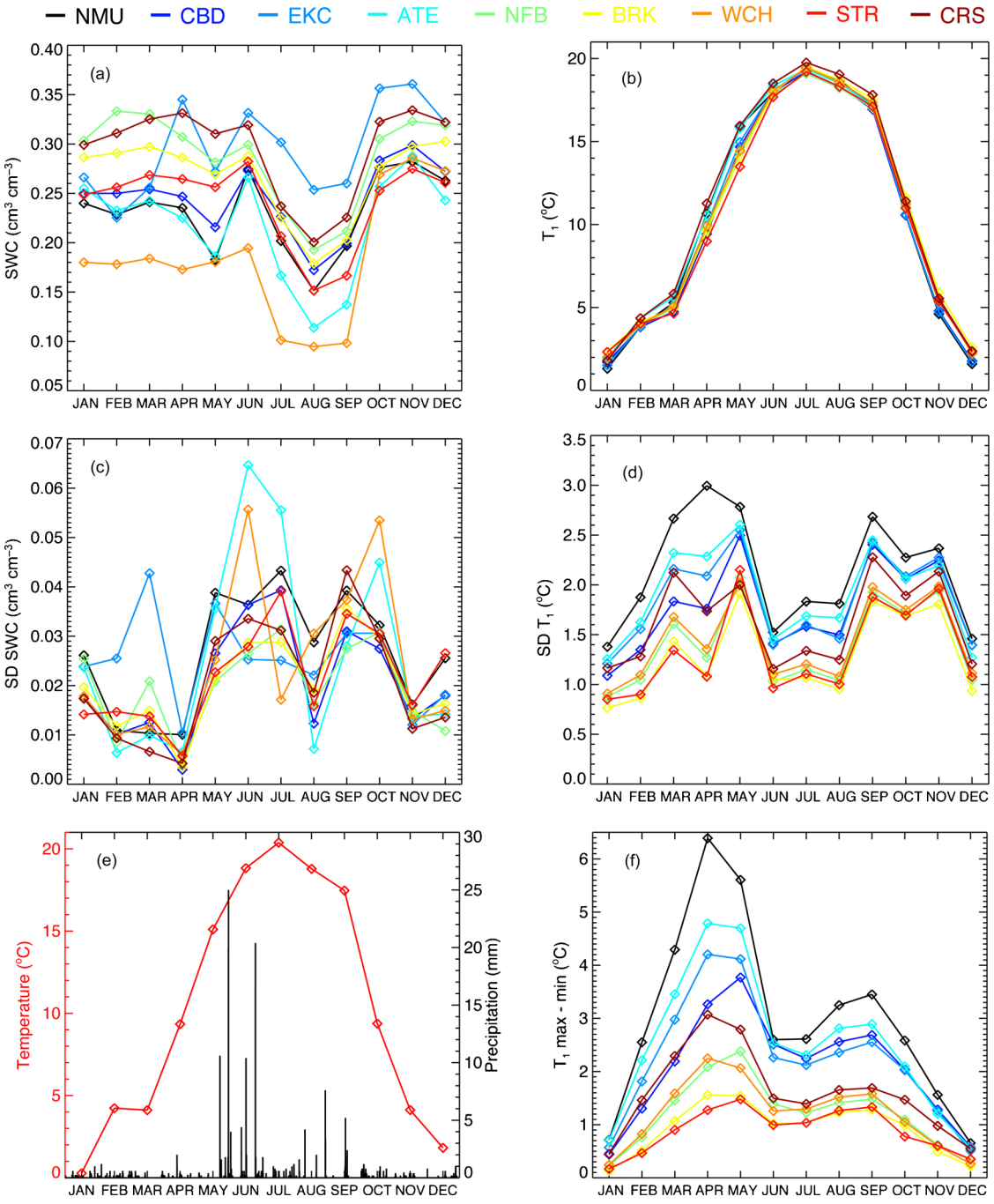

Fig. 2. Monthly mean values of soil temperature – T_1 (a) and soil water content (SWC) (b) (per each mulch variant), their sigma values (c, d), mean day range of soil temperature T_1 maximum minus T_1 minimum (f), monthly mean values of air temperatures (e), and precipitation amount (e). NMU–Not mulched control patch; CBD–Cardboard; EKC–EkoCover RF– decomposable foil; ATE–Agrotex EKO + decomposable matting; NFB–Polypropylene nonwoven fabric covered bark chips layer; BRK–Bark chips; WCH–Wood chips; STR–Wheat straw; CRS–Crushed stone.

water regime within the soil sample (i.e., the cumulative outflow in time and the points of the retention curves) was simulated using the single-porosity model in HYDRUS-1D (Šimůnek et al., 2016), and the parameters of the van Genuchten (1980) soil hydraulic functions were optimized via a numerical inversion:

$$\theta_e = \frac{\theta - \theta_r}{\theta_s - \theta_r}\,,\ \theta_e = \frac{1}{(1 + (\alpha\ |h|)^n)^m}\,,\ h < 0,\ \ \theta_e = 1,\ h \geq 0 \tag{2}$$

$$K(\theta) = K_s \theta_e^{\lambda} [1 - (1 - \theta_e^{1/m})]^2\,,\ h < 0\,,\ K(\theta) = K_s\,,\ h \geq 0 \tag{3}$$

where θ_e is the effective soil water content (dimensionless), θ_r and θ_s are the residual and saturated soil water contents [$L^3\ L^{-3}$], respectively, h is the pressure head [L], α is the reciprocal of the absolute value of the air-entry pressure head [L^{-1}], n (dimensionless) is related to the slope of the retention curve at the inflection point, m = 1 – 1 / n, K_s is the saturated hydraulic conductivity [$L\ T^{-1}$], and λ is the pore-connectivity parameter (dimensionless). The pore connectivity parameter was set at an average value for many soils (λ = 0.5) (Mualem, 1976). The saturated soil water contents (θ_s) equaled to measured values and were fixed in the numerical inversion. Parameters θ_r, α, n and K_s were optimized. The goodness of fit was assessed using the coefficient of determination (R^2), root mean square weighted error (RMSE)

and Akaike information criterion (AIC), which varied between 0.9919 and 0.9995 (R^2), 0.0101 and 0.0329 (RMSE), and -728.4 and -333.1 (AIC). Next the absolute value of the negative pressure head, h_{inf}, soil water content, θ_{inf}, and curve slope, S_{inf}, at the inflection point (Dexter, 2004a,b,c; Dexter and Czyz, 2007) were calculated as follows:

$$h_{\text{inf}} = \frac{1}{\alpha}\left(\frac{1}{m}\right)^{\frac{1}{n}} \quad (4)$$

$$\theta_{\text{inf}} = (\theta_s - \theta_r)\left(1 + \frac{1}{m}\right)^{-m} + \theta_r \quad (5)$$

$$S_{\text{inf}} = -n(\theta_s - \theta_r)\left(1 + \frac{1}{m}\right)^{-(1+m)} \quad (6)$$

Additionally, the gravitational water (GW) and readily available water (RAW) were expressed in mm of water per 1 cm soil layer as follows:

$$GW = (\theta_s - \theta_{100})^* 10 \quad (7)$$

$$RAW = (\theta_{100} - \theta_{250})^* 10 \quad (8)$$

where θ_{100} and θ_{250} are the soil water contents for the pressure heads of -100 and −250 cm, respectively.

After performing the multistep outflow tests, soil samples were oven dried at 105 °C until constant weight had been achieved and the bulk densities (ρ_d) were evaluated using a standard method (Dane and Topp, 2002).

2.5. Data analysis

The STATISTICA 13.3 software (StatSoft Inc., USA) was used to perform statistical analyses. First, the normality of all data sets was tested (Kolmogorov-Smirnov and Liliefors test). Outliers (based on the three-sigma rule of thumb (Upton and Cook, 2008)) of each variable were excluded from the dataset. The basic statistical parameters, such as the mean and coefficient of variation (the ratio of the standard deviation to the mean; the statistical measure of the dispersion of data points in a data series around the mean), were computed. A main effect analysis of variance (mANOVA) was used to analyses the first-order effect of multiple categorical independent variables (year and mulch). A Fisher multiple range test was computed for the categorical variables (95.0 % LSD (least significant difference)). Basic relationships among the soil properties were assessed by correlation analysis. The Correlation coefficient matrix was expanded with information about significance at different probability levels. Based on the correlation analysis results, which showed relationships among the studied variables, values of the basic soil characteristics and retention curve parameters were treated with a factor analysis.

3. Results and discussion

3.1. Soil water and thermal regimes

Soil chemical and physical parameters could be influenced directly by mulch material itself (i.e., its permeability, chemical composition, or decomposition rate) or indirectly by alternated microclimatic conditions below the mulch layer, which can influence many processes taking place in soils (e.g., chemical reactions, dissolution or precipitation of various substances, their movement, swelling and shrinking of clay particles, root growth and distribution, edaphon activity). To illustrate trends and variability of soil water contents and temperatures (T_1) measured in 2016, mean values and standard deviations (SD) were calculated for each month. In addition, monthly means of daily temperature ranges (differences between daily maximal and minimal temperatures) were evaluated (Fig. 2). Fig. 2 also shows mean monthly air temperatures and daily precipitation amounts monitored at the experimental station in Prague-Troja (http://www.emsbrno.cz/p.axd/cs/Troja.CZUKZ.html).

Soil water contents corresponded to the precipitation distribution during the year (i.e., soil water contents increased) and plant transpiration demands (i.e., high root water uptake during the summer time resulted in low water contents). The vegetation effects upon soil water dynamics and on the relationship between vegetation and soil moisture variation with season have been documented among others by Fan et al. (2015) and Ni et al. (2019). Initially, soil water contents were mostly higher than those measured for the control variant, which shows an effective preservation of water in soils. Interestingly, under wood chips initially measured values were lower than those for the control variant. The reason could be that the fresh wooden material captured during the first year (2015) more precipitation than other organic materials and thus less water reached soil surface. During the year 2016 this material was largely degraded and likely therefore measured water contents were at the end of 2016 similar to those under other organic materials. Responses during the summer season were mainly affected by plant root water uptake (Jacobs et al., 2011). The differences in soil water contents monitored for various mulches are uneasily interpreted because of high data variability documented by SD values. Especially in the case of foils EKC and ATE, SD values were high in some months. They could be explained by a low permeability of both foils, accumulation of precipitated water at their surfaces and an occasional leakage of accumulated water through the foil perforation for TMS3 installation.

In contrast, soil temperature distribution during the year well documented the differences among mulch variants. In general, in the beginning (February – June) the higher average temperatures were measured under crushed stone, followed by average temperatures monitored under bare surface (control patches without mulch), foil mulches and organic mulches. Later on (July – September) average temperatures were similar with exception of crushed stone and at the end of the year temperatures measured under bare surface and foil mulches were lower than under other materials. The highest daily ranges of soil temperature were observed in control patches without mulch, lower ranges below foils mulches, followed by crushed stone, and the lowest were below organic mulches. Similarly, Kodešová et al. (2014) also documented different average temperatures and daily temperature oscillations under different surface covers. They showed temperatures under bark chips being lower and higher than those under gravel and sand mulching during the spring and summer period, and winter, respectively. They also documented low daily temperature

Fig. 3. Perennials cover development during vegetation season. April (A); June (B); July (C); October (D).

ranges under bark chips and higher under gravel and sand materials. These differences are mainly due to different abilities of the surface materials to reflect or adsorb solar radiation (bare soil or mulch) or energy emitted from the soil surface (mulch), and differences in heat capacity (faster exchange for materials of lower heat capacity), thermal conductivity (faster exchange for materials of higher thermal conductivity) and thickness (faster exchange for materials of lower thickness) of the mulch materials (Al-Shammary et al., 2020; Bonachela et al., 2020; Dietrich et al., 2019; Kodešová et al., 2014; Zhang et al., 2017; Zhou et al., 2020). During the vegetation season ranges and SD values (Fig. 3) followed vegetation development. They were highest in spring before vegetation integration. Effect of mulch was higher than vegetation effect. After that, during summer months with integrated vegetation soil cover, amplitudes and sigma values decreased. In September, perennials were cut and both values again increased. Also, Zhang et al. (2020) and Duan et al. (2019) found that with the increase of vegetation density, mean daily minimum soil temperature reduced significantly and mean diurnal soil temperature ranges became smaller. Zhang et al. (2017) showed that the net radiation and consequently soil heat flux and temperature differed for different soil covers, but under canopy this impact was reduced or completely diminished.

Increased soil temperature can also affect soil organism communities and below-ground biological processes, including the dynamics of soil organisms (Briones et al., 2009). An effect of increasing soil temperature on plant growth rate was documented by Jacobs et al. (2011). Higher soil moisture and lower temperature fluctuation afforded by the organic mulching were associated with increases in the microorganism abundance (Almeida et al., 2011). Dietrich et al. (2019) presented a direct relationship of the mulch thickness (straw) and the moisture and decomposition rate of the underlying layers. Microorganisms' activity afterwards can influence soil pH or stability of soil structure and consequently hydraulic properties.

3.2. Mulch and time impacts on soil properties

The soil properties and parameters of the soil hydraulic functions measured under different soil covers are shown in Figs. 4 and 5, respectively (mean values and standard deviations) and in Appendix B (Tables B1 and B2, the mean values and coefficients of variation). By mANOVA (Table 3), a highly significant time effect (the differences among studied years: 2015, 2016, 2017, 2018 respectively) was found only in the distribution of several soil properties, and the mulch effect (the differences among mulches in the whole studied period) was found in the distribution of almost all soil properties. The values of pH_{H2O} were found to be highly variable during the study period.

3.2.1. Basic soil characteristics and soil aggregate stability

Fig. 4 and Appendix B – Table B1 (which also includes a denotation of significant differences among mulch types separately for the each year) show that after the first growing season, the soils under the biodegradable foils (ATE and EKC), including cardboard, had a lower pH_{CaCl2} than others, but significance of the differences was decreased by higher data variability in 2015. Saglam et al. (2017) showed that both biodegradable paper and biodegradable plastic mulches reduced evaporation. However, this effect depended on their disintegration rates during the growing season (Moreno et al., 2017). The decrease of pH could be explained by the relatively impermeable cover of soil and consequently by the reduction in CO_2 emission. CO_2 originates from soil respiration. Part of the CO_2 can be transformed to carbonic acid. This, in turn, promotes plant growth through CO_2 fertilisation, and may have further stimulated root development and increased the exudation of organic acids (Steinmetz et al., 2016). After disruption of the compact cover (after the second planting season), this effect vanished. We also conclude that pH_{CaCl2} was significantly lower under the bark chips in 2016 and 2018. The decomposition of bark or general tree litter can increase soil acidity, as documented in many studies (e.g. Pohlman and McColl, 1988; van Hees et al., 2001; Pavlů et al., 2018). Muñoz et al. (2017) documented a soil pH decrease also under straw mulch, but this decrease was not observed in our results. Enhanced acidification could contribute to nutrient depletion and thus to decreased crop production (Gupta et al., 2013).

The distribution of C_{ox} (Fig. 4 and Appendix B – Table B1) was relatively homogeneous in the first two years. There were no differences among mulches or between years. For instance, Muñoz et al. (2017) also showed that soil organic carbon did not differ significantly between treatments (straw and plastic mulching) after three years. However, in our case, C_{ox} content decreased in almost all mulch variants during 2017 (except bark and wood chip patches); this could be likely ascribed to generally lower plant biomass production in the third and fourth seasons (data will be published separately by aforementioned gardening research group). The C_{ox} content in the soils under bark and wood chips maintained stable or increased (i.e., the highest values were in 2018) because of the carbon supply from decomposing mulch. On the other hand, C_{ox} did not increase under straw mulching, even though this material could also be a source of organic carbon. For instance, Blanco-Canqui and Lal (2007) showed that straw mulching after 10 years significantly increased soil organic carbon at the top layer of a Stagnic Luvisol developed on a loamy till. This could be explained firstly by the 10 year period, which yielded a larger amount of straw application than our case, and secondly by the different soil textures (i.e., the light sandy loam and silt loam in our and their study, respectively), followed by the greater mobility of decomposed organic matter in our soil compared to that in their poorly drained soil.

After the first planting season, the soil structure stability evaluated using the WSA index (Fig. 4 and Appendix B – Table B1) was lowest at the control patch without mulch, where soil was exposed to the mechanical impact of raindrops. Cambardella and Elliott (1993) showed that a reduction of this mechanical disturbance of soil contributes to a higher proportion of water stable aggregates. It has been shown that soil aggregate stability and soil structure can be improved when mulch cover is applied to the soil's surface (Stirzaker and White, 1995; Walsh et al., 1996). Our result only partially confirms this statement. The WSA index increased during the study period under natural mulches (bark/wood chips and straw) but did not considerably change (and even slightly decreased) under other mulches.

Higher soil aggregate stability usually results in more stable intra-aggregate fine porosity that enhances water retention, increases soil water infiltration capacity, and thus increases soil resistance to detachment by overland flow (Kong et al., 2005; Mulumba and Lal, 2008). An increase of soil aggregate stability under straw mulch was also documented by Mulumba and Lal (2008).

3.2.2. Soil hydraulic properties

Fig. 5 and Appendix B – Table B2 show that bulk density values (ρ_d) were significantly higher in 2015 than in 2018. Correspondingly, all soil water contents, saturated, residual, and water content at the inflection point (θ_s, θ_r, and θ_{inf}) were significantly lower in 2015 than in 2018. The α values and the saturated hydraulic conductivities (K_s) were significantly lower in 2015 than those in 2018. The absolute values of the negative pressure heads at the inflection point (h_{inf}) were higher in 2015 than in 2018 (Table 3). These changes were due to the development of the soil structure (i.e., the initial consolidation, swelling, and shrinking during the wetting and drying cycles, root growth, zooedaphon activity, etc.), which resulted in higher proportion of large capillary pores that are typical for untilled soils as in grasslands (Fér et al., 2016; Kodešová et al., 2011a) and some garden soils (Koestel and Schlüter, 2019). Later development of these soils is mainly affected by soil flora and fauna activities. Fér et al. (2020), who studied change of the same hydro-physical characteristics in the agricultural field after twelve years with no-tillage practice showed that the soil water

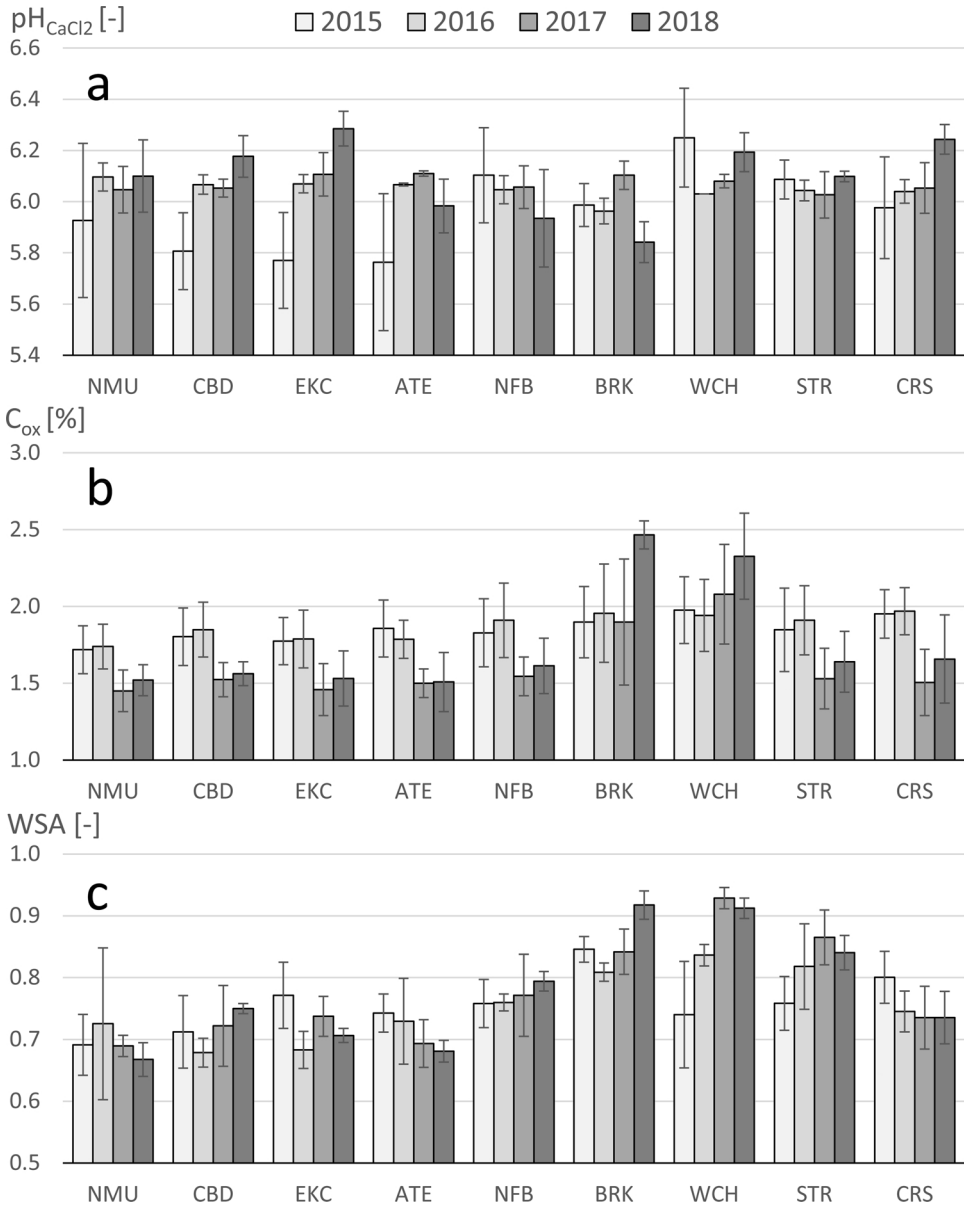

Fig. 4. Mean values (per each mulch variant) of (**a**) pH_{CaCl2}, (**b**) organic carbon content (C_{ox}), and (**c**) the water stable aggregate index (WSA) in years 2015–2018. Error bars indicate standard deviations. NMU–Not mulched control patch; CBD–Cardboard; EKC–EkoCover RF– decomposable foil; ATE–Agrotex EKO+ decomposable matting; NFB–Polypropylene nonwoven fabric covered bark chips layer; BRK–Bark chips; WCH–Wood chips; STR–Wheat straw; CRS–Crushed stone.

retention capacity represented by the saturated soil water content and the reciprocal of the air-entry pressure head was higher in the no-tillage field than in the conventional tillage field. The soil physical quality represented by the slope of the soil water retention curve at the inflection point was also better under no-tillage. In addition, Fér et al. (2020) showed that the hydraulic conductivity at the pressure head of −2 cm measured using the mini disk tension infiltrometer was higher in the no-tillage than in the conventional tillage field. On the other hand, an ambiguous effect of no-till farming on soil physical and hydraulic properties was summarized by Skaalsveen et al. (2019). Reviewed studies frequently documented increased topsoil compaction, reduced porosity and high bulk density under no-till practice in comparison to that under conventional tillage. However, several studies showed that soil structure under no-till farming could be improved considerably by introducing cover crops, but root and canopy characteristics of the cover crop are crucial to the achieve the desired effect.

Corresponding to the optimized van Genuchten parameters, the mean soil water retention (SWRC) and hydraulic conductivity (HCC) curves of variously mulched soils (Fig. 6) show different trends for the year 2015 than for 2018, as well as trends under different soil covers. In 2015, SWRCs seem to have been more variable than SWRCs in 2018. There was no similarity among the SWRCs of soils under similar mulch materials (e.g., foils and organic materials), except for a very similar trend of SWRCs from non-mulched control plots (NMU) and plots with cardboard (CBD). In the case of HCCs, similar shapes of HCCs were observed for soils under organic mulches (BRK, WVH, and STR) and for NMU and CBD. The reasons for this phenomenon could be that the soil was not fully consolidated after 6 months, and the influence of various covers was too short. This variability could be partially ascribed to natural soil variability after soil loosening and perennials outplanting.

In 2018, the SWRCs were less variable. However, the trends of the SWRC under comparable materials were similar. For instance, the SWRCs were similar for soils under foils EKC, ATE, and NFB (despite their decomposition during the initial 2 years), and organic materials

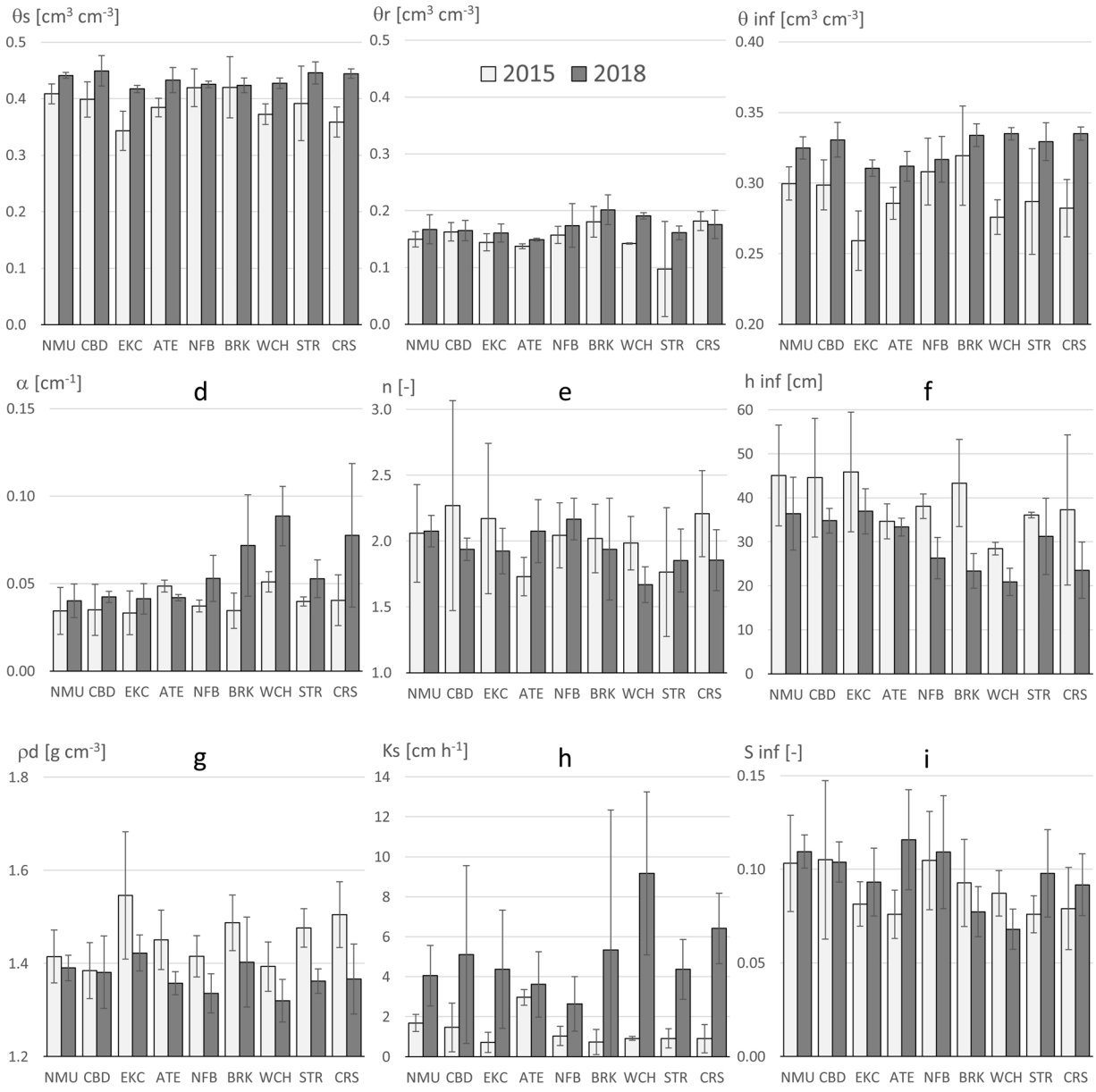

Fig. 5. Mean values (per each mulch variant) of (**a**) saturated soil water contents–θ_s, (**b**) residual soil water contents–θ_r, (**c**) soil water content at the inflection point–θ_{inf}, (**d**) parameter α, (**e**) parameter n, (**f**) absolute value of the negative pressure head at the inflection point–h_{inf}, (**g**) bulk density–ρ_d, (**h**) saturated hydraulic conductivity–K_s, and (**i**) retention curve slope at the inflection point–S_{inf} in years 2015 and 2018. Error bars indicate standard deviations. NMU–Not mulched control patch, CBD–Cardboard, EKC–EkoCover RF–decomposable foil, ATE–Agrotex EKO + decomposable matting, NFB–Polypropylene nonwoven fabric covered bark chips layer, BRK–Bark chips, WCH–Wood chips, STR–Wheat straw, and CRS–Crushed stone.

such as bark (BRK) and wood (WCH) chips (but not for wheat straw (STR), which was more similar to the effects under crushed stone (CRS)). Fig. 5 and Appendix B – Table B2 show that the reciprocal value of the air-entry pressure head (α) was the lowest at the control patches or below the decomposable foils during different stages of decomposition (the EkoCover RF foil and card board were completely decomposed in 2016, while the Agrotex ECO + matting still persisted). The highest α value was that below the wood chips. Bark chips and crushed stones also attained high values, but the significance of this difference was reduced by higher data variability. An opposite trend was shown for the absolute value of the pressure head at the inflection point (h_{inf}). The higher values were observed in the control plots and in plots with decomposable foils, and the lower values were in plots with bark and wood chips and also with crushed stones. The highest values for water contents at inflection points were those for soils below wood chips and crushed stones, and the lowest values were for soils below EkoCover RF and Agrotex ECO + . Soil below wood chips was also characterized by the lowest value of the curve slope in the inflection point (S_{inf}). The behaviour of K_s was related to the mulch type but, the significance of these differences has been reduced by the higher data variability. Similar HCC trends were again observed for BRK and WCH, and for EKC, ATE, and NFB. In 2018, the SWRC and HCC from the control plots were, again, similar to the SWRC from plots with cardboard, which indicated no influence from cardboard, the fastest decomposable material, on the SWRC.

The resulting values of the curve slope in the inflection point (S_{inf}) in all cases indicated a very good physical quality of soils ($S_{inf} > 0.05$, (Dexter, 2004a,b,c; Dexter and Czyz, 2007)). However, contrary to the improvement of organic matter content and aggregate stability in soils under the organic mulches the physical quality of these soils decreased

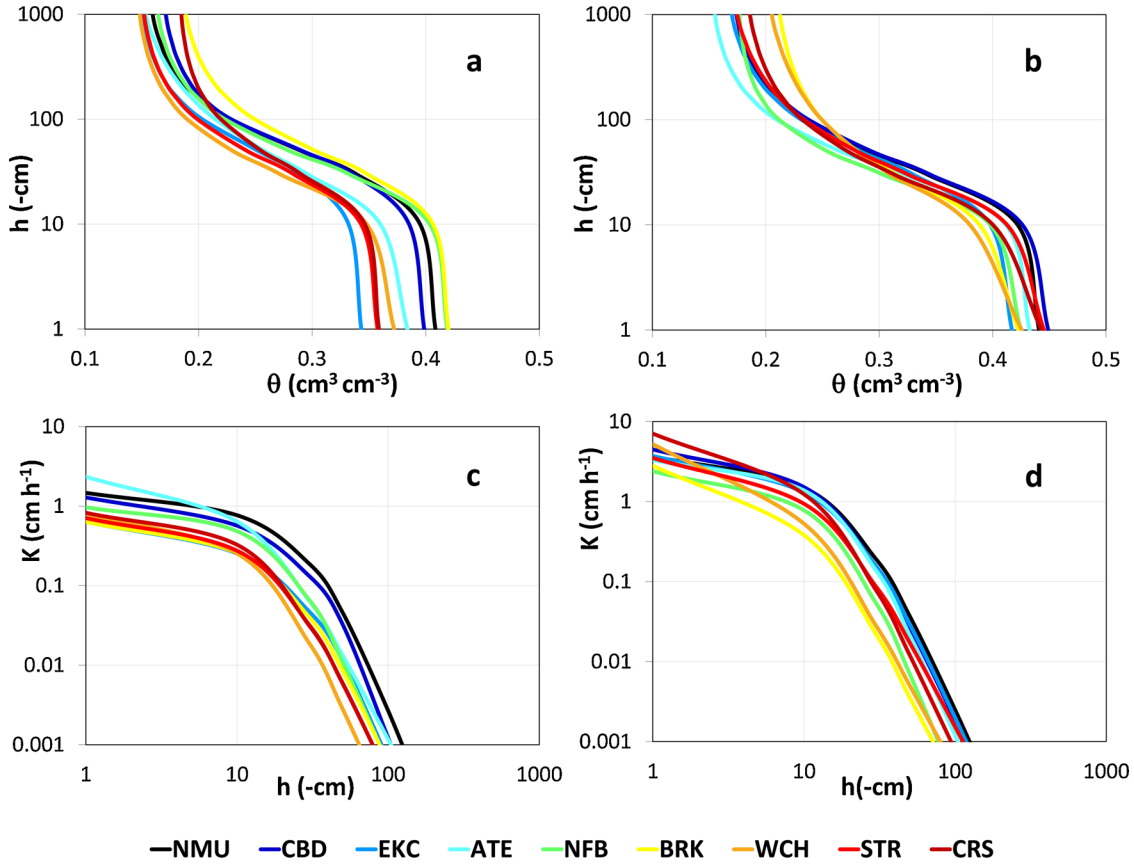

Fig. 6. Mean soil water retention (SWRC) and hydraulic conductivity (HCC) curves of the soils under various mulches: NMU–Not mulched control patch, CBD–Cardboard, EKC–EkoCover RF–decomposable foil, ATE–Agrotex EKO + decomposable matting, NFB–Polypropylene nonwoven fabric covered bark chips layer, BRK–Bark chips, WCH–Wood chips, STR–Wheat straw, and CRS–Crushed stone; (**a**) SWRC in 2015, (**b**) SWRC in 2018, (**c**) HCC in 2015, and (**d**) HCC in 2018; θ is the volumetric soil water content, h is the soil water pressure head and K is the hydraulic conductivity.

(i.e. the S_{inf} values were lower in these soils compared to other soils). This effect could be caused by a migration of organic matter elements into soil pores and thus reduction of their size. Similar trends were observed in the case of evaluated values of GW and RAW (Fig. 7). Comparing years 2015 and 2018 the amounts of the gravitational water increased almost in all cases except BRK and WCH, in which were similar. The amounts of readily available water were mostly similar, except NFB, BRK and WCH. In these soils RAWs indicated aggravation of plant water accessibility.

3.3. Relationships among soil parameters

Interrelationships among basic soil characteristics and soil hydraulic parameters were first evaluated by correlation analysis. The analysis did not confirm any statistically significant relationships between those properties when assuming data from 2015 due to slower response of soil hydraulic parameters to mulching in comparison to the chemical properties. However, in case of data from 2018, a significant relationship between C_{ox} content and aggregate stability was proven (Table 4),

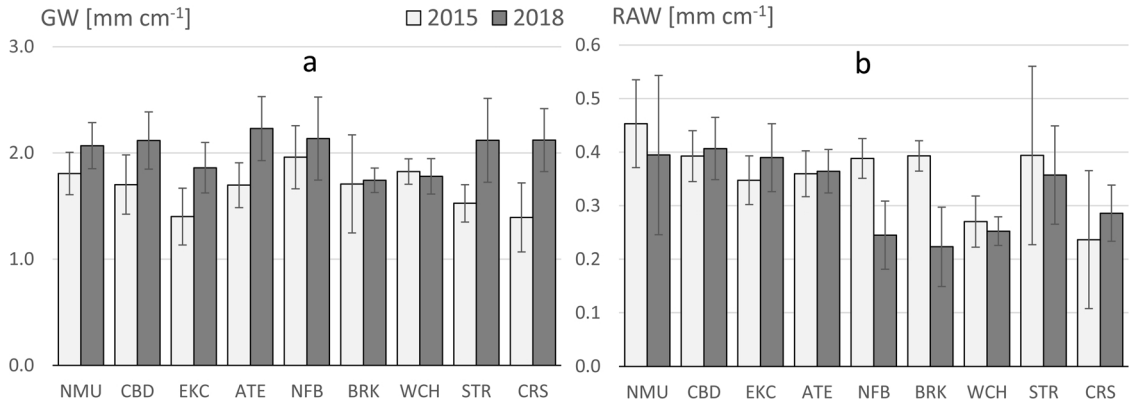

Fig. 7. Mean values (per each mulch variant) of (**a**) gravitational water (GW) and (**b**) readily available water (RAW). Error bars indicate standard deviations. NMU–Not mulched control patch, CBD–Cardboard, EKC–EkoCover RF–decomposable foil, ATE–Agrotex EKO + decomposable matting, NFB–Polypropylene nonwoven fabric covered bark chips layer, BRK–Bark chips, WCH–Wood chips, STR–Wheat straw, and CRS–Crushed stone.

Table 4
Correlation coefficients of the relationships among the studied soil properties from the year 2018. (pH in H_2O or $CaCl_2$ soil extract, organic carbon content (C_{ox}), water stable aggregate index (WSA), saturated soil water content (θ_s), residual soil water content (θ_r), parameters α and n, saturated hydraulic conductivity (Ks), absolute value of the negative pressure head at the inflection point (h_{inf}), soil water content at the inflection point (θ_{inf}), retention curve slope at the inflection point (S_{inf}), bulk density (ρ_d), gravitational water (GW), and readily available water (RAW).

Variable	pH_{H2O}	pH_{CaCl2}	C_{ox}	WSA	θ_s	θ_r	α	n	K_s	h_{inf}	θ_{inf}	S_{inf}	ρ_d	GW	RAW
pH_{H2O}	1														
pH_{CaCl2}	0.864***	1													
C_{ox}	−0.231	−0.235	1												
WSA	−0.182	−0.243	0.825***	1											
θ_s	0.283	0.156	−0.336	−0.129	1										
θ_r	−0.202	−0.362	0.536**	0.445*	−0.271	1									
α	−0.015	0.005	0.607**	0.523**	−0.071	0.294	1								
n	−0.237	−0.371	−0.500**	−0.400*	0.084	0.012	−0.637***	1							
K_s	0.230	0.270	0.254	0.135	0.193	−0.003	0.813***	−0.668***	1						
h_{inf}	0.221	0.263	−0.574**	−0.561**	0.042	−0.492**	−0.848***	0.254	−0.538**	1					
θ_{inf}	0.113	−0.068	0.397*	0.435*	0.506**	0.606**	0.461*	−0.303	0.424*	−0.498**	1				
S_{inf}	0.002	−0.068	−0.733***	−0.542**	0.473*	−0.531**	−0.642***	0.792***	−0.469*	0.427*	−0.374	1			
ρd	−0.012	−0.001	−0.192	−0.237	−0.248	0.151	−0.513**	0.432*	−0.497**	0.486*	−0.236	0.186	1		
GW	0.077	0.047	−0.597***	−0.367	0.689***	−0.624***	−0.241	0.472*	−0.055	0.085	−0.156	0.858***	−0.195	1	
RAW	0.403*	0.491**	−0.509**	−0.487**	0.322	−0.702***	−0.546**	−0.120	−0.139	0.853***	−0.313	0.314	0.129	0.221	1

*, **, *** represent significant correlation at α = 0.05, 0.01, and 0.001, respectively.

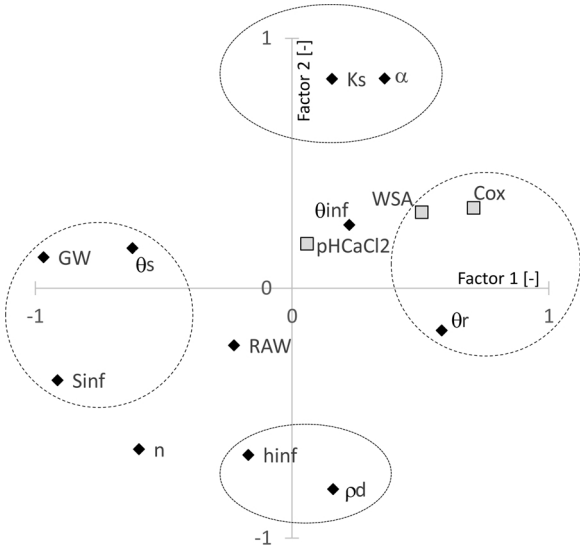

Fig. 8. Results of the factor analysis. Plot of loadings of the 1 st and 2nd factors explaining 32 % respectively 23 % of the variability in the original data. Displayed variables: basic soil characteristics (grey squares)–pH_{CaCl2}, organic carbon content (C_{ox}), water stable aggregate index (WSA) and bulk density (ρ_d); hydraulic conductivity and van Genuchten parameters (black diamonds)–saturated hydraulic conductivity (K_s), saturated soil water contents (θ_s), residual soil water contents (θ_r), soil water content at the inflection point (θ_{inf}), parameters α and n, absolute value of the negative pressure head at the inflection point (h_{inf}), and retention curve slope at the inflection point (S_{inf}), gravitational water (GW), and readily available water (RAW).

as in many previous studies (e.g., Jakšík et al., 2015; Kodešová et al., 2009; Zádorová et al., 2011). In contrast, Nzeyimana et al. (2017) showed that an increase in the soil organic carbon content after mulching did not directly stabilise the soil structure. This stabilisation was more influenced by the composition of organic compounds. The contribution of plant-derived biomolecules, such as lignin and microbial-derived compounds (amino sugars), was discussed (Angst et al., 2017).

Highly significant correlations among α, K_s, and h_{inf} complemented the higher mentioned distribution of these parameters among mulch variants. K_s increased with an increase in α, and both K_s and α increased with a decrease in h_{inf}. These relationships associate with the fact that the air entry pressure head (its absolute value is a reciprocal of α) influences the position of the inflection point. Low absolute values of the air entry pressure head and h_{inf} indicate a higher volume of large pores and thus a higher K_s. The strongest relationship between basic soil characteristics and retention curve parameters was found between the C_{ox} content and S_{inf}. The value of S_{inf} decreased (i.e., soil physical quality decreased) with an increase in C_{ox}, which was in contrast to expectations that C_{ox} should improve soil structure (i.e., the soil's physical quality that was discussed above). Similarly, S_{inf} negatively correlated with WSA. The reason for this negative correlation could be that elements of organic matter migrate into soil pores and reduce their size, thereby resulting in lower water contents for pressure heads between 0 and -h_{inf} and higher water contents for pressure heads below -h_{inf}. The statistical analysis was also carried out with data from both soil core sampling years (2015 and 2018). This analysis in some cases showed similar but less significant correlations among parameters (Appendix B – Table B3) due to the different trends in temporal changes of different properties to various mulch materials. Resulted statistical parameters were mainly controlled by data from 2018.

The interrelationships among soil properties, van Genuchten parameters, and derived SWRC characteristics were also proven using a factor analysis (Fig. 8). Four factors (Varimax normalized) were extracted, and these factors accounted for 85 % of the variability in the

original data. The first factor (28 % of the variability) described interrelationships among WSA, C_{ox}, θ_r, θ_s, n, $S_{inf,}$ and GW. The second factor (24 % of the variability) described the interrelationships among ρ_d, n, h_{inf}, K_s, and α. The third factor accounted for 20 % of the variability, and the highest factor loadings showed variables pH_{CaCl2}, θ_r, h_{inf}, and RAW. The fourth factor (12 % of the variability) described the indirect relationship between θ_s, and θ_{inf}.

4. Conclusions

The results of our study answered all questions asked in the introduction. They document the significant time-dependent changes of the chemical and physicochemical soil properties under different mulch types. The fastest response to the changes at the soil surface (i.e., after the application of different soil covers) was observed for the soil pH, which decreased during the first planting season. The lowest pH was under the decomposable foils (before their disintegration), probably due to a reduction of CO_2 emission. This effect vanished after the foil disruption. The largest effect of mulching was found in the case of the organic carbon and aggregate stability under organic mulches (straw, bark chips, and wood chips). The increase in C_{ox} well correlated with the increase of the aggregate stability. On the other hand, the soil hydraulic properties considerably changed in all patches mainly due to the no-till practices during the 4-year-period. Except BRK and WCH, all derived parameters mostly indicated the improvement of the soil's hydraulic physical quality (i.e., improved pore diversification, ensuring water retention, as well as aeration and increased hydraulic conductivity controlling water infiltration). In the cases of the organic mulches (BRK and WCH), the retention curve slope at the inflection point (S_{inf}) indicated aggravation of soil physical quality. Due to the different trends in temporal changes of different properties to various mulch materials, the statistically significant relations between the C_{ox} content and the parameters of the van Genuchten functions and the characteristics of the SWRC inflection points were found only for data obtained in 2018. The SWRCs' shapes of soils under the bark and wood chips were more gradual than those for soils under other mulching materials and control (e.g., higher values of α and θ_r and lower values of S_{inf} were found in the soils under the bark and wood chips compared to these values for other soils). Some similarities in the shapes of SWRC were observed for the soil under different mulching foils or matting. However, the SWRC parameters did not largely differ from the parameters of remaining soils. Similar trends were observed for HCCs. This suggests that organic mulches have largest and long-time impact on soil chemical parameters (carbon content) that also affect aggregate stability, soil water retention curves, and hydraulic properties. Generally, organic mulches offer more benefits for soil in comparison with foil mulches. They are natural sources of organic matter, are permeable and not limiting soil gas circulation, do not bring any xenobiotics into soil nature, and enhance soil structure stability, nevertheless seem to reduce RAW, in particular BRK. However, for entirely objective conclusions, it must be stated that effects of mulch materials, especially degradable straw, bark and wood chips, on soil properties may differ over a much longer period. Besides, the results may be different for other soil types and different root and canopy characteristics. The impact of mulch on soil structural properties should be investigated in greater detail using for instance X-ray micro-tomography, etc.

Appendix A

(See Fig. A1).

Appendices

A Fig. A1: Experimental design; **B** Table B1: Mean values (per each mulch variant) of pH_{H2O}, pH_{CaCl2}, organic carbon concentration (C_{ox}) and water stable aggregate index (WSA) in years 2015 – 2018. Table contains also coefficient of variation and results of analysis of variance, Table B2: Mean values (per each mulch variant) of saturated soil water contents – θ_s, residual soil water contents – θ_r, reciprocal value of the air-entry pressure head – α, slope of the retention curve at the inflection point – n, saturated hydraulic conductivity – K_s, absolute value of the negative pressure head at the inflection point – h_{inf}, soil water content at the inflection point – θ_{inf}, retention curve slope at the inflection point – $S_{inf,}$ and bulk density – ρ_d, in years 2015 and 2018. Table contains also coefficient of variation and results of analysis of variance. Table B3: Correlation coefficients of the relationships among the studied soil properties from the years 2015 and 2018: pH in H_2O or $CaCl_2$ soil extract, organic carbon content (C_{ox}), water stable aggregate index (WSA), saturated soil water contents (θ_s), residual soil water contents (θ_r), parameters α and n, saturated hydraulic conductivity (K_s), absolute value of the negative pressure head at the inflection point (h_{inf}), soil water content at the inflection point (θ_{inf}), and retention curve slope at the inflection point (S_{inf}).

Declaration of Competing Interest

The authors declare that they have no known competing financial interests or personal relationships that could have appeared to influence the work reported in this paper.

Acknowledgments

Authors acknowledge the financial support of the European Structural and Investment Funds, Operational Programme Research Development and Education Project NutRisk Centre (No. CZ.02.1.01/0.0/0.0/16_019/0000845). Special thanks go to staff of university experimental station in Troja.

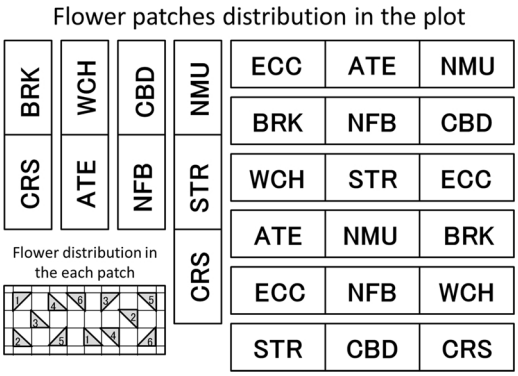

Fig. A1. Experimental design – patches with different mulches in three replications (NMU–Not mulched control patch, CBD–Cardboard, EKC–EkoCover RF– decomposable foil, ATE–Agrotex EKO + decomposable matting, NFB–Polypropylene nonwoven fabric covered bark chips layer, BRK–Bark chips, WCH–Wood chips, STR–Wheat straw, CRS–Crushed stone) and flower distribution in square plantation spacing (1. *Geranium sanguineum* 'Ankum´s Pride', 2. *Hemerocallis* 'Stella D´Oro', 3. *Salvia nemorosa* 'Caradonna', 4. *Echinacea purpurea* 'Primadonna Deep Rose', 5. *Coreopsis verticilata* 'Grandiflora', 6. *Heuchera sanguinea* 'Leuchtkäfer').

Appendix B

Table B1
Mean values (per each mulch variant) of pH_{H2O}, pH_{CaCl2}, organic carbon concentration (C_{ox}) and water stable aggregate index (WSA) in years 2015 – 2018. Table contains also coefficient of variation (CV, ratio of the standard deviation to the mean) and results of analysis of variance (95 % LSD, letters a, b, c in columns represent homogeneous groups (h.g)); NMU–Not mulched control patch, CBD–Cardboard, EKC–EkoCover RF– decomposable foil, ATE–Agrotex EKO + decomposable matting, NFB–Polypropylene nonwoven fabric covered bark chips layer, BRK–Bark chips, WCH–Wood chips, STR–Wheat straw, CRS–Crushed stone.

year	mulch	pH_{H2O}			pH_{CaCl2}			C_{ox} [%]			WSA		
		mean	h.g.	CV	mean	h.g.	CV	mean	h.g.	CV	mean	h.g.	CV
2015	NMU	6.78	bc	4.21	5.93	abc	5.08	1.72	a	9.05	0.69	c	7.13
2015	CBD	6.63	c	1.44	5.81	bc	2.59	1.80	a	10.38	0.71	c	8.25
2015	EKC	6.63	c	1.29	5.77	bc	3.25	1.77	a	8.63	0.77	abc	6.94
2015	ATE	6.71	bc	1.78	5.76	c	4.64	1.86	a	9.97	0.74	bc	4.15
2015	NFB	6.85	abc	1.72	6.10	ab	3.04	1.83	a	12.10	0.76	bc	5.15
2015	BRK	6.88	ab	1.10	5.99	abc	1.40	1.90	a	12.22	0.85	a	2.46
2015	WCH	7.08	a	1.59	6.25	a	3.09	1.98	a	10.97	0.74	bc	11.66
2015	STR	6.94	ab	0.65	6.09	abc	1.24	1.85	a	14.71	0.76	bc	5.73
2015	CRS	6.92	ab	1.89	5.98	abc	3.32	1.95	a	8.11	0.80	ab	5.24
2016	NMU	6.56	a	2.05	6.10	a	0.90	1.74	a	8.37	0.73	bc	16.92
2016	CBD	6.53	a	0.77	6.07	a	0.62	1.85	a	9.64	0.68	c	3.44
2016	EKC	6.59	a	0.53	6.07	a	0.59	1.79	a	10.53	0.68	c	4.40
2016	ATE	6.54	a	1.04	6.07	a	0.10	1.79	a	6.93	0.73	bc	9.54
2016	NFB	6.54	a	1.10	6.05	a	0.91	1.91	a	12.68	0.76	abc	1.79
2016	BRK	6.53	a	1.54	5.96	b	0.84	1.96	a	16.38	0.81	ab	1.82
2016	WCH	6.56	a	0.18	6.03	ab	0.00	1.94	a	12.08	0.84	a	2.06
2016	STR	6.53	a	0.93	6.04	a	0.67	1.91	a	11.79	0.82	ab	8.46
2016	CRS	6.53	a	0.55	6.04	a	0.76	1.97	a	7.82	0.75	abc	4.42
2017	NMU	6.76	ab	1.65	6.05	a	1.50	1.45	c	9.32	0.69	e	2.50
2017	CBD	6.46	c	1.05	6.05	a	0.58	1.52	bc	7.30	0.72	de	9.03
2017	EKC	6.88	a	1.14	6.11	a	1.39	1.46	c	11.60	0.74	de	4.40
2017	ATE	6.87	ab	2.11	6.11	a	0.16	1.50	c	6.21	0.69	e	5.58
2017	NFB	6.76	ab	0.09	6.06	a	1.37	1.55	bc	8.13	0.77	cd	8.62
2017	BRK	6.69	ab	1.80	6.10	a	0.90	1.90	ab	21.61	0.84	bc	4.35
2017	WCH	6.76	ab	2.60	6.08	a	0.44	2.08	a	15.59	0.93	a	1.86
2017	STR	6.81	ab	3.33	6.03	a	1.51	1.53	bc	12.92	0.87	ab	5.13
2017	CRS	6.65	bc	1.85	6.05	a	1.63	1.51	c	14.36	0.74	de	6.91
2018	NMU	6.96	ab	1.96	6.10	bc	2.31	1.52	b	6.68	0.67	f	4.08
2018	CBD	6.92	ab	1.83	6.18	ab	1.32	1.56	b	4.92	0.75	de	1.09
2018	EKC	6.99	a	2.87	6.29	a	1.08	1.53	b	11.75	0.71	ef	1.62
2018	ATE	6.78	bcd	1.43	5.98	cd	1.76	1.51	b	12.71	0.68	f	2.57
2018	NFB	6.70	cd	2.33	5.94	cd	3.20	1.61	b	11.18	0.79	c	2.00
2018	BRK	6.64	d	0.96	5.84	d	1.37	2.47	a	3.71	0.92	a	2.49
2018	WCH	7.05	a	0.99	6.19	ab	1.23	2.33	a	12.03	0.91	a	1.82
2018	STR	6.88	abc	0.44	6.10	bc	0.34	1.64	b	12.10	0.84	b	3.32
2018	CRS	7.01	a	1.14	6.24	ab	0.92	1.66	b	17.31	0.74	de	5.77

Table B2

Mean values (per each mulch variant) of saturated soil water contents – θ_s, residual soil water contents – θ_r, reciprocal value of the air-entry pressure head – α, slope of the retention curve at the inflection point – n, saturated hydraulic conductivity – K_s, absolute value of the negative pressure head at the inflection point – h_{inf}, soil water content at the inflection point – θ_{inf}, retention curve slope at the inflection point – $S_{inf,}$ and bulk density – ρ_d, in years 2015 and 2018. Table contains also coefficient of variation (CV, ratio of the standard deviation to the mean) and results of analysis of variance (95 % LSD, letters a, b, c in columns represent homogeneous groups (h.g)); NMU–Not mulched control patch, CBD–Cardboard, EKC–EkoCover RF– decomposable foil, ATE–Agrotex EKO + decomposable matting, NFB–Polypropylene nonwoven fabric covered bark chips layer, BRK–Bark chips, WCH–Wood chips, STR–Wheat straw, CRS–Crushed stone.

year	variant	θ_s [cm^3cm^{-3}]			θ_r [cm^3cm^{-3}]			α [cm^{-1}]			n [-]			K_s[cm h^{-1}]		
		mean	h.g.	CV	mean	h.g.	CV	mean	h.g.	CV	mean	h.g.	CV	mean	h.g.	CV
2015	NMU	0.41	a	4.34	0.15	ab	9.15	0.03	ab	39.05	2.06	a	18.03	1.68	b	25.65
2015	CBD	0.40	ab	7.86	0.16	a	9.91	0.03	ab	41.73	2.27	a	35.15	1.46	b	83.80
2015	EKC	0.34	b	10.11	0.14	ab	10.41	0.03	b	37.57	2.17	a	26.37	0.72	b	70.41
2015	ATE	0.38	ab	4.22	0.14	ab	3.15	0.05	ab	6.93	1.73	a	8.49	2.96	a	13.11
2015	NFB	0.42	a	8.01	0.16	a	9.58	0.04	ab	9.05	2.04	a	12.10	1.03	b	46.47
2015	BRK	0.42	a	12.90	0.18	a	14.92	0.03	ab	29.45	2.02	a	12.90	0.73	b	86.14
2015	WCH	0.37	ab	4.90	0.14	ab	0.97	0.05	ab	11.25	1.98	a	10.29	0.91	b	10.88
2015	STR	0.39	ab	16.86	0.10	b	86.34	0.04	ab	6.33	1.76	a	27.72	0.91	b	52.75
2015	CRS	0.36	ab	7.46	0.18	a	9.26	0.04	a	36.00	2.21	a	14.77	0.90	b	79.72
2018	NMU	0.44	ab	1.16	0.17	abc	15.37	0.04	c	23.93	2.07	a	5.75	4.05	b	37.44
2018	CBD	0.45	a	5.95	0.17	abc	10.79	0.04	c	7.64	1.94	ab	4.41	5.10	ab	87.19
2018	EKC	0.42	b	1.53	0.16	bc	9.93	0.04	c	21.10	1.92	ab	8.97	4.37	ab	67.78
2018	ATE	0.43	ab	5.15	0.15	c	1.66	0.04	c	4.11	2.08	a	11.54	3.61	b	45.38
2018	NFB	0.43	ab	1.37	0.17	abc	22.08	0.05	bc	24.92	2.17	a	7.30	2.64	b	51.87
2018	BRK	0.42	ab	3.07	0.20	a	13.10	0.07	abc	40.46	1.94	ab	19.94	5.33	ab	131.53
2018	WCH	0.43	ab	2.18	0.19	ab	2.83	0.09	a	19.12	1.67	b	8.14	9.17	ab	44.44
2018	STR	0.45	a	4.43	0.16	bc	7.50	0.05	bc	20.56	1.85	ab	12.95	4.37	ab	34.28
2018	CRS	0.44	a	1.82	0.18	abc	14.27	0.08	ab	52.83	1.85	ab	12.47	6.41	a	27.49

year	variant	h_{inf} [cm]			θ_{inf} [cm^3cm^{-3}]			S_{inf} [-]			ρ_d [g cm^{-3}]			GW [mm cm^{-1}]			RAW [mm cm^{-1}]		
		mean	h.g.	CV	mean	h.g.	CV	mean	h.g.	CV	mean	h.g.	CV	mean	h.g.	CV	mean	h.g.	CV
2015	NMU	45.08	ab	25.37	0.30	ab	3.92	0.10	a	25.00	1.41	b	4.00	1.81	ab	11.09	0.45	a	18.08
2015	CBD	44.57	ab	30.30	0.30	abc	5.93	0.11	a	40.27	1.38	b	4.35	1.70	ab	16.36	0.39	ab	12.08
2015	EKC	45.88	ab	29.62	0.26	c	8.12	0.08	a	14.63	1.55	a	8.85	1.40	b	19.08	0.35	abc	13.09
2015	ATE	34.66	ab	11.44	0.29	abc	3.99	0.08	a	17.01	1.45	ab	4.42	1.70	ab	12.46	0.36	abc	11.95
2015	NFB	38.09	ab	7.29	0.31	ab	7.70	0.10	a	25.13	1.42	b	3.11	1.96	a	15.17	0.39	ab	9.60
2015	BRK	43.36	ab	22.91	0.32	a	11.03	0.09	a	25.12	1.49	ab	4.02	1.71	ab	27.05	0.39	ab	7.17
2015	WCH	28.46	b	4.99	0.28	bc	4.45	0.09	a	13.97	1.39	b	3.82	1.82	ab	6.51	0.27	bc	17.69
2015	STR	36.07	a	1.69	0.29	abc	13.01	0.08	a	13.07	1.48	ab	2.82	1.53	ab	11.52	0.39	ab	42.29
2015	CRS	37.24	ab	45.87	0.28	abc	7.20	0.08	a	27.74	1.50	ab	4.69	1.39	b	23.37	0.24	c	54.39
2018	NMU	36.39	a	22.66	0.32	abc	2.44	0.11	ab	8.15	1.39	ab	1.98	2.07	ab	4.04	0.39	ab	32.36
2018	CBD	34.78	ab	8.11	0.33	ab	3.73	0.10	ab	10.28	1.38	ab	5.63	2.12	ab	13.76	0.41	a	15.26
2018	EKC	36.92	a	13.91	0.31	c	1.89	0.09	abc	19.52	1.42	a	2.74	1.86	ab	8.80	0.39	ab	14.33
2018	ATE	33.34	ab	6.07	0.31	c	3.38	0.12	a	23.07	1.36	ab	1.85	2.23	a	14.91	0.36	cd	11.38
2018	NFB	26.29	bcd	17.76	0.32	bc	5.11	0.11	ab	27.64	1.34	ab	3.15	2.14	ab	19.04	0.25	d	18.79
2018	BRK	23.39	cd	16.95	0.33	ab	2.42	0.08	bc	17.26	1.40	ab	6.90	1.74	b	4.62	0.22	cd	30.09
2018	WCH	20.90	d	14.94	0.33	a	1.31	0.07	c	15.83	1.32	b	3.49	1.78	ab	8.90	0.25	abc	9.82
2018	STR	31.24	abc	27.81	0.33	ab	4.06	0.10	abc	23.93	1.36	ab	1.91	2.12	ab	19.66	0.36	abc	28.17
2018	CRS	23.53	cd	27.21	0.33	a	1.41	0.09	abc	18.01	1.37	ab	5.49	2.12	ab	9.73	0.29	bcd	14.15

Table B3
Correlation coefficients of the relationships among the studied soil properties from the years 2015 and 2018: pH in H_2O or $CaCl_2$ soil extract, organic carbon content (C_{ox}), water stable aggregate index (WSA), saturated soil water content (θ_s), residual soil water content (θ_r), parameters α and n, saturated hydraulic conductivity (Ks), absolute value of the negative pressure head at the inflection point (h_{inf}), soil water content at the inflection point (θ_{inf}), retention curve slope at the inflection point (S_{inf}), bulk density (ρ_d), gravitational water (GW), and readily available water (RAW).

Variable	pH_{H2O}	pH_{CaCl2}	C_{ox}	WSA	θ_s	θ_r	α	n	K_s	h_{inf}	θ_{inf}	S_{inf}	ρ_d	GW	RAW
pH_{H2O}	1														
pH_{CaCl2}	0.872***	1													
C_{ox}	−0.100	−0.114	1												
WSA	−0.059	−0.078	0.683***	1											
θ_s	0.245	0.373**	−0.098	0.048	1										
θ_r	−0.025	0.035	0.196	0.259	0.079	1									
α	0.079	0.162	0.417**	0.410**	0.253	0.204	1								
n	−0.053	−0.090	−0.248	−0.233	−0.192	0.367**	−0.520***	1							
K_s	0.208	0.228	0.175	0.273*	0.458**	0.195	0.730***	−0.400**	1						
h_{inf}	−0.090	−0.187	−0.268	−0.323*	−0.371**	−0.250	−0.810***	0.473***	−0.501***	1					
θ_{inf}	0.203	0.326*	0.121	0.241	0.929***	0.353**	0.414**	−0.212	0.546***	−0.463***	1				
S_{inf}	0.124	0.179	−0.500***	−0.376**	0.416**	0.087	−0.433**	0.704***	−0.167	0.249	0.210	1			
ρ_d	−0.239	−0.357**	−0.059	−0.056	−0.621***	−0.128	−0.471***	0.112	−0.596***	0.468***	−0.591***	−0.272*	1		
GW	0.213	0.357**	−0.388**	−0.182	0.759***	0.055	0.169	0.074	0.298*	−0.416**	0.574**	0.683***	−0.604***	1	
RAW	0.112	0.103	−0.302*	−0.336*	0.241	−0.553***	−0.502***	−0.141	−0.108	0.685***	0.018	0.214	0.037	0.025	1

*, **, *** represent significant correlation at α = 0.05, 0.01, and 0.001, respectively.

References

Almeida, D.D.O., Klauberg Filho, O., Almeida, H.C., Gebler, L., Felipe, A.F., 2011. Soil microbial biomass under mulch types in an integrated apple orchard from Southern Brazil. Sci. Agric. 68, 217–222.

Al-Shammary, A.A.G., Kouzani, A., Gyasi-Agyei, Y., Gates, W., Rodrigo-Comino, J., 2020. Effects of solarisation on soil thermal-physical properties under different soil treatments: a review. Geoderma 363, 114137.

Angst, G., Mueller, K.E., Kögel-Knabner, I., Freeman, K.H., Mueller, C.W., 2017. Aggregation controls the stability of lignin and lipids in clay-sized particulate and mineral associated organic matter. Biogeochemistry 132 (3), 307–324.

Blanco-Canqui, H., Lal, R., 2007. Soil structure and organic carbon relationships following 10 years of wheat straw management in no-till. Soil Tillage Res. 95, 240–254.

Blasing, M., Amelung, W., 2018. Plastics in soil: analytical methods and possible sources. Sci. Total Environ. 612, 422–435.

Bonachela, S., López, J.C., Granados, M.R., Magán, J.J., Hernández, J., Baille, A., 2020. Effects of gravel mulch on surface energy balance and soil thermal regime in an unheated plastic greenhouse. Biosyst. Eng. 192, 1–13. https://doi.org/10.1016/j.biosystemseng.2020.01.010.

Briones, M.J.I., Ostle, N.J., McNamara, N.P., Poskitt, J., 2009. Functional shifts of grassland soil communities in response to soil warming. Soil Biol. Biochem. 41 (2), 315–322.

Cambardella, C.A., Elliott, E.T., 1993. Carbon and nitrogen distribution in aggregates from cultivated and native grassland soils. Soil Sci. Soc. Am. J. 57, 1071–1076.

Casagrande, A., 1934. Die Aräometer-Methode zur Bestimmung der Kornverteilung von Böden und anderen Materialien. J. Springer, Berlin.

Dane, J.H., Topp, C.T., 2002. Methods of Soil Analysis, Part 4 — Physical Methods. Soil Science Society of America, Inc., Madison.

Dexter, A.R., 2004a. Soil physical quality. Part I. Theory, effect of soil texture, density and organic matter, and effect on root growth. Geoderma 120, 201–214.

Dexter, A.R., 2004b. Soil physical quality. Part II. Friability, tillage, tilth and hardsetting. Geoderma 120, 215–226.

Dexter, A.R., 2004c. Soil physical quality. Part III. Unsaturated hydraulic conductivity and general conclusions about S-theory. Geoderma 120, 227–239.

Dexter, A.R., Czyz, E.A., 2007. Application of S-theory in study of soil physical degradation and its consequences. Land Degrad. Dev. 18, 369–381.

Dietrich, G., Recous, S., Pinheiro, P.L., Weiler, D.A., Schu, A.L., Rambo, M.R.L., Giacomini, S.J., 2019. Gradient of decomposition in sugarcane mulches of various thicknesses. Soil Tillage Res. 192, 66–75.

Doran, J.W., 1980. Microbial changes associated with residue management with reduced tillage. Soil Sci. Soc. Am. J. 44, 518–524.

Duan, M., Xie, J., Mao, X., 2019. Modeling water and heat transfer in soil-plant-atmosphere continuum applied to maize growth under plastic film mulching. Front. Agric. Sci. Eng. 6 (2), 144–161.

Fan, J., Baumgartl, T., Scheuermann, A., Lockington, D.A., 2015. Modeling effects of canopy and roots on soil moisture and deep drainage. Vadose Zone J. 14 (2), 27–33.

Fér, M., Kodešová, R., Nikodem, A., Jirků, V., Jakšík, O., Němeček, K., 2016. The impact of the permanent grass cover or conventional tillage on hydraulic properties of Haplic Cambisol developed on paragneiss substrate. Biologia 71 (10), 1144–1150.

Fér, M., Kodešová, R., Hroníková, S., Nikodem, A., 2020. The effect of 12-year ecological farming on the soil hydraulic properties and repellency index. Biologia 75, 795–798.

Gale, W.J., Mc Coil, R.W., Fang, X., 1993. Sandy fields traditional farming for water conservation in China. J. Soil Water Conserv. 48, 474–477.

Gupta, N., Gaurav, S.S., Kumar, A., 2013. Molecular basis of aluminium toxicity in plants: a review. Am. J. Plant Sci. 4, 21–37.

International Organization of Standardization, 2005. Soil Quality - Determination of pH. (ISO 10390:2005).

IUSS, 2014. World Reference Base for Soil Resources 2014. World Soil Resources Reports No. 106. FAO, Rome.

Jacobs, A.F.G., Heusinkveld, B.G., Holtslag, A.A.M., 2011. Long-term record and analysis of soil temperatures and soil heat fluxes in a grassland area, the Netherlands. Agric. For. Meteorol. 151, 774–780.

Jakšík, O., Kodešová, R., Kubiš, A., Stehlíková, I., Drábek, O., Kapička, A., 2015. Soil aggregate stability within morphologically diverse areas. Catena 127, 287–299.

Kader, M.A., Senge, M., Mojid, M.A., Ito, K., 2017a. Recent advances in mulching materials and methods for modifying soil environment. Soil Tillage Res. 168, 155–166.

Kader, M.A., Senge, M., Mojid, M.A., Nakamura, K., 2017b. Mulching type-induced soil moisture and temperature regimes and water use efficiency of soybean under rain-fed condition in central Japan. Int. Soil Water Conserv. Res. 5, 302–308.

Kasirajan, S., Ngouajio, M., 2012. Polyethylene and biodegradable mulches for agricultural applications: a review. Agron. Sustain. Dev. 32, 501–529.

Kodešová, R., Rohošková, M., Žigová, A., 2009. Comparison of aggregate stability within six soil profiles under conventional tillage using various laboratory tests. Biologia 64, 550–554.

Kodešová, R., Jirků, V., Kodeš, V., Mühlhanselová, M., Nikodem, A., Žigová, A., 2011a. Soil structure and soil hydraulic properties of Haplic Luvisol used as Arable Land and Grassland. Soil Tillage Res. 111 (2), 154–161.

Kodešová, R., Kodeš, V., Mráz, A., 2011b. Comparison of two sensors ECH2O EC-5 and SM200 for measuring soil water content. Soil Water Res. 6 (2), 102–110.

Kodešová, R., Fér, M., Klement, A., Nikodem, A., Teplá, D., Neuberger, P., Bureš, P., 2014. Impact of various surface covers on water and thermal regime of Technosol. J. Hydrol. 519, 2272–2288.

Koestel, J., Schlüter, S., 2019. Quantification of the structure evolution in a garden soil over the course of two years. Geoderma 338, 597–609.

Kong, A.Y.Y., Six, J., Bryant, D.C., Denison, R.F., van Kessel, C., 2005. The relationships

between carbon input, aggregation, and soil organic carbon stabilization in sustainable cropping systems. Soil Sci. Soc. Am. J. 69, 1078–1085.
Lemon, E.R., 1956. Potentialities for decreasing soil moisture evaporation loss. Soil Sci. Soc. Am. Proc. 20, 120–125.
Li, Y., Hu, Y., Song, D., Liang, S., Qin, X., Siddique, K.H.M., 2019. The effects of straw incorporation with plastic film mulch on soil properties and bacterial community structure on the loess plateau. Eur. J. Soil Sci. 2019, 1–16.
Ma, Y.M., Li, Y.X., 2011. Water accumulation in soil by gravel and sand mulches: influence of textural composition and thickness of mulch layers. J. Arid Environ. 75, 432–437.
Moreno, M.M., Gonzalez-Mora, S., Villena, J., Campos, J.A., Moreno, C., 2017. Deterioration pattern of six biodegradable, potentially low-environmental impact mulches in field conditions. J. Environ. Manage. 200, 490–501.
Mualem, Y., 1976. A new model for predicting the hydraulic conductivity of unsaturated porous media. Water Resour. Res. 12 (3), 513–522.
Mulumba, L.N., Lal, R., 2008. Mulching effects on selected soil physical properties. Soil Tillage Res. 98, 106–111.
Muñoz, K., Buchmann, C., Meyer, M., Schmidt-Heydt, M., Steinmetz, Z., Diehl, D., Thiele-Bruhn, S., Schaumann, G.E., 2017. Physicochemical and microbial soil quality indicators as affected by the agricultural management system in strawberry cultivation using straw or black polyethylene mulching. Appl. Soil Ecol. 113, 36–44.
Nachtergaele, J., Poesen, J., van Wesemael, B., 1998. Gravel mulching in vineyards of southern Switzerland. Soil Tillage Res. 46, 51–59.
Ni, J.J., Ni, Junjun, Cheng, Y., Wang, Q., ChWW, Ng, Garg, A., 2019. Effects of vegetation on soil temperature and water content: field monitoring and numerical modelling. J. Hydrol. 571, 494–502.
Nimmo, J.R., Perkins, K.S., 2002. Aggregate stability and size distribution. In: Dane, J.H., Topp, G.C. (Eds.), Methods of Soil Analysis, Part 4 – Physical Methods. Soil Science Society of America, Inc., Madison, USA, pp. 317–328.
Nzeyimana, I., Hartemink, A.E., Ritsema, C., Stroosnijder, L., Lwanga, E.H., Geissen, V., 2017. Mulching as a strategy to improve soil properties and reduce soil erodibility in coffee farming systems of Rwanda. Catena 149, 43–51.
Pavlů, L., Drábek, O., Stejskalová, Š., Tejnecký, V., Hradilová, M., Nikodem, A., Borůvka, L., 2018. Distribution of Aluminium fractions in acid forest soils: influence of vegetation changes. iForest 11, 721–727.
Pohlman, A.A., McColl, J.G., 1988. Soluble organics from forest litter and their role in metal dissolution. Soil Sci. Soc. Am. J. 52, 265–271.
Qiu, Y., Xie, Z., Wang, Y., Ren, J., Malhi, S.S., 2014. Influence of gravel mulch stratum thickness and gravel grain size on evaporation resistence. J. Hydrol. 519, 1908–1913.
Rees, H.W., Chow, T.L., Loro, P.J., Lavoie, J., Monteith, J.O., Blaauw, A., 2002. Hay mulching to reduce runoff and soil loss under intensive potato production in northwestern New Brunswick, Canada. Can. J. Soil Sci. 82 (2), 249–258.
Saglam, M., Sintim, H.Y., Bary, A.I., Miles, C.A., Ghimire, S., Inglis, D.A., Flury, M., 2017. Modeling the effect of biodegradable paper and plastic mulch on soil moisture dynamics. Agric. Water Manag. 193, 240–250.
Šimůnek, J., van Genuchten, M.T., Šejna, M., 2016. Recent developments and applications of the HYDRUS computer software packages. Vadose Zone J. 15 (7). https://doi.org/10.2136/vzj2016.04.0033.
Skaalsveen, K., Ingram, J., Clarke, L.E., 2019. The effect of no–till farming on the soil functions of water purification and retention in North–western Europe: a literature review. Soil Tillage Res. 189, 98–109.
Smets, T., Poesen, J., Knapen, A., 2008. Spatial scale effects on the effectiveness of organic mulches in reducing soil erosion by water. Earth-Sci. Rev. 89, 1–12.
Sparks, D.L., 1996. Methods of Soil Analysis, Part 3 – Chemical Methods SSSA Book Series: 5. Soil Science Society of America, American Society of Agronomy, Inc., Madison.
Steinmetz, Z., Wollmann, C., Schaefer, M., Buchmann, Ch., David, J., Tröger, J., Muñoz, K., Frör, O., Schaumann, G.E., 2016. Plastic mulching in agriculture. Trading short-term Agronomic benefits for long-term soil degradation? Sci. Total Environ. 550, 690–705.
Stirzaker, R.J., White, I., 1995. Amelioration of soil compaction by a cover-crop for no-tillage lettuce production. Aust. J. Agric. Res. 46 (3), 553–568.
Subrahmaniyan, K., Zhou, W.J., 2008. Soil temperature associated with degradable, non-degradable plastic and organic mulches and their effect on biomass production, enzyme activities and seed yield of winter rapeseed (Brassica napus L.). J. Sustain. Agric. 32, 611–627.
Upton, G., Cook, I., 2008. A Dictionary of Statistics, 2nd ed. rev. Oxford University Press, Oxford.
van Dam, J.C., Stricker, N.N., Droogers, P., 1994. Inverse method to determine soil hydraulic function from multi-step outflow experiment. Soil Sci. Soc. Am. J. 58, 647–652.
van Genuchten, M.T., 1980. A closed-form equation for predicting the hydraulic conductivity of unsaturated soils. Soil Sci. Soc. Am. J. 44, 892–898.
van Hees, P.A.W., Tipping, E., Lundström, U.S., 2001. Aluminium speciation in forest soil solution—modelling the contribution of low molecular weight organic acids. Sci. Total Environ. 278, 215–229.
Walsh, B.D., Salmins, S., Buszard, D.J., MacKenzie, A.F., 1996. Impact of soil management systems on organic dwarf apple orchards and soil aggregate stability, bulk density, temperature and water content. Can. J. Soil Sci. 76 (2), 203–209.
Wang, J., Liu, X., Li, Y., Powell, T., Wang, X., Wang, G., Zhang, P., 2019. Microplastics as contaminants in the soil environment: a mini-review. Sci. Tot. Environ. 691, 848–857.
Wild, J., Kopecký, M., Macek, M., Šanda, M., Jankovec, J., Haase, T., 2019. Climate at ecologically relevant scales: a new temperature and soil moisture logger for long-term microclimate measurement. Agri. For. Meteorol. 268, 40–47.
Xie, Z., Wanga, Y., Cheng, G., Malhi, S.S., Vera, C.L., Guo, Z., Zhang, Z., 2010. Particle-size effects on soil temperature, evaporation, water use efficiency and watermelon yield in fields mulched with gravel and sand in semi-arid Loess Plateau of northwest China. Agric. Water Manag. 97, 917–923.
Yang, Y., Li, P., Jiao, J., Yang, Z., Lv, M., Li, Y., Zhou, Ch., Wang, Ch., He, Z., Liu, Y., Song, S., 2020. Renewable sourced biodegradable mulches and their environment impact. Sci. Hortic. 268, 109375.
Yuan, C., Lei, T., Mao, L., Liu, H., Wu, Y., 2009. Soil surface evaporation processes under mulches of different sized gravel. Catena 78, 117–121.
Zádorová, T., Jakšík, O., Kodešová, R., Penížek, V., 2011. Influence of terrain attributes and soil properties on soil aggregate stability. Soil Water Res. 6, 111–119.
Zhang, Y.L., Wang, F.X., Shock, C.C., Yang, K.J., Kang, S.Z., Qin, J.T., Li, S.E., 2017. Eff ;ects of plastic mulch on the radiative and thermal conditions and potato growth under drip irrigation in arid Northwest China. Soil Tillage Res. 172, 1–11.
Zhang, Y.L., Wang, F.X., Shock, C.C., Feng, S.Y., 2020. Modeling the interaction of plastic film mulch and potato canopy growth with soil heat transport in a semiarid area. Agronomy 10, 190.
Zhou, L., Zhao, W., He, J., Flerchinger, G.N., Feng, H., 2020. Simulating soil surface temperature under plastic film mulching during seedling emergence of spring maize with the RZ–SHAW and DNDC models. Soil Till. Res. 197, 104517.